Revised and Accepted proof, Applied Surface Science (January 2015)

High N-content a-C:N films elaborated by femtosecond PLD with plasma assistance

C. Maddi[a], C. Donnet[a*], A.-S. Loir[a], T. Tite[a], V. Barnier[b], T.C. Rojas[c], J.C. Sanchez-Lopez[c], K. Wolski[b], F. Garrelie[a]

[a]*Université de Lyon, F-69003, Lyon, France, Université de Saint-Étienne, Laboratoire Hubert Curien (UMR 5516 CNRS), 42000 Saint-Étienne, France*

[b]*Laboratoire Georges Friedel, Ecole Nationale Supérieure des Mines, 42023 Saint-Etienne, France*

[c]*Instituto de Ciencia de Materiales de Sevilla (CSIC-US), Avda. Américo Vespucio 49, 41092 Sevilla, Spain*

*Corresponding author: Prof. Christophe DONNET (C. Donnet), Hubert Curien Laboratory, UMR CNRS 5516, Saint Etienne, 42000, France, Tel: +33 4 77 91 58 05, Fax: +33 4 77 91 57 81

E-mail address: Christophe.Donnet@univ-st-etienne.fr

Abstract

Amorphous carbon nitride (a-C:N) thin films are a interesting class of carbon-based electrode materials. Therefore, synthesis and characterization of these materials have found lot of interest in environmental analytical microsystems. Herein, we report the nitrogen-doped amorphous carbon thin film elaboration by femtosecond pulsed laser deposition (fs-PLD) both with and without a plasma assistance. The chemical composition and atomic bonding configuration of the films were investigated by multi-wavelength (MW) Raman spectroscopy, X-ray photoelectron spectroscopy (XPS) and electron energy-loss spectroscopy (EELS). The highest nitrogen content, 28 at.%, was obtained with plasma assistance. The I(D)/I(G) ratio and the G peak position increased as a function of nitrogen concentration, whereas the dispersion and full width at half maximum (FWHM) of G peak decreased. This indicates more ordered graphitic like structures in the films both in terms of topological and structural, depending on the nitrogen content. EELS investigations were correlated with MW Raman results. The interpretation of XPS spectra of carbon nitride films remains a challenge. Plasma assisted PLD in the femtosecond regime led to a significant high nitrogen concentration, which is highlighted on the basis of collisional processes in the carbon plasma plume interacting with the nitrogen plasma.

Keywords: Carbon nitride, plasma assistance, femtosecond laser, PLD, XPS, EELS, MW Raman spectroscopy

Acronyms: a-C- amorphous carbon, a-C:N- amorphous carbon nitride, biased a-C:N-DC plasma assistance deposited amorphous carbon nitride

1. Introduction

In the last decade, the deposition of higher nitrogen content amorphous carbon films received specific attention following the theoretical prediction of a hypothetical C_3N_4 phase isostructural to β-Si_3N_4 whose hardness might be equal or superior to that of diamond [1, 2]. Although the synthesis of such crystalline C_3N_4 compound was not successful the resulting amorphous CN (a-C:N) materials found applications in optical and magnetic storage technology as protective coatings [3, 4]. In particular, it is found that a higher nitrogen incorporation has a beneficial effect on electronic properties and its use as electrode material [5-10] as well as many other potential applications [11].

The properties of amorphous carbon nitride coatings strongly depend on the deposition methods [4, 12-14], since various types of chemical and physical vapor deposition techniques have been used (including hybrid coating processes), such as radio frequency plasma enhanced chemical vapor deposition (RF PECVD) eventually carried with direct current (DC) magnetron sputtering [4, 13], ion beam assisted cathodic arc deposition [15], filtered pulsed cathodic arc deposition [16, 17], pulsed laser deposition (PLD) [10, 12, 18], DC magnetron sputtering [19] and electrochemical deposition [20]. Among the above mentioned techniques, the PLD is a promising way to deposit carbon nitride films with enhanced physical, chemical and electrochemical properties because it can be easily carried out even on non-conductive substrates and at low substrate temperatures during film growth. Up to now, most of the works deal with the deposition of a-C:N films by nanosecond pulsed laser deposition [12, 21, 22]. Recent studies have shown the ability to dope amorphous carbon (a-C) materials by femtosecond pulsed laser deposition (fs-PLD) [18, 23] but nitrogen doped a-C films deposited by femtosecond PLD, in particular with plasma assistance, is still largely unexplored. Such investigation may be paramount for the synthesis of a-C:N films with significantly higher nitrogen contents, typically in the 20-50 at.% range. Muhl *et al.* [24] reviewed the deposition methods for carbon nitride films and pointed out that to overcome this limitation, atomic or ionic nitrogen should be used to bombard the film surface during the deposition process. Reactive plasma is an effective way to enhance the ionization of the gas molecules. DC glow discharge with proper bias voltage improve the N content in films [25-28]. Moreover this method is easier to operate compared to other atomic and ion sources. Thus the coupling of direct current plasma assistance with femtosecond laser ablation is of prime interest and will be developed in the present paper.

Many researchers characterized the a-C:N materials by different techniques. X-ray photoelectron spectroscopy (XPS) has been used extensively to study the chemical bonding configurations [4, 12, 13, 15, 16, 18, 29-30, 32, 41-45] with however a still controversial identification of carbon and nitrogen bonding configurations. Therefore, it is obvious that complementary additional techniques are important to obtain a more complete knowledge of a-C:N films. On the one hand, the electron energy-loss spectroscopy (EELS)

provides useful information regarding the bonding character of the films [29, 30], on the other hand, Raman spectroscopy is a standard and non-destructive technique widely used for the characterization of all kinds of carbon-based materials.

In this paper, we emphasize the advantages of using reactive PLD over the conventional PLD in terms of N content and CN bonds formation. The effect of deposition conditions on the chemical composition and atomic bonding structure of the carbon nitride films is studied by X-ray photoelectron spectroscopy (XPS) combined with EELS and MW Raman spectroscopy in order to obtain consistent conclusions on the bonding structure of carbon and nitrogen in a-C:N films with various nitrogen contents tailored by plasma assistance of the femtosecond PLD process.

2. Experimental

Amorphous carbon nitride thin films were prepared by femtosecond pulsed laser deposition (fs-PLD) with and without the assistance of DC discharge plasma. Deposition of films is performed at room temperature by ablating a graphite target onto silicon (Si) substrates. A femtosecond laser system working at 800 nm wavelength, with pulse duration of 60 fs and a repetition rate of 1 kHz was used. The laser beam was focused at an angle of 45 ° onto a high purity graphite target (99.9995% purity). The substrates were mounted on sample holder at a distance of 36 mm from the target. High purity (99.9995%) N_2 gas was used as the reactant gas. A DC source was used to generate a plasma of nitrogen into the chamber. The negative electrode of the DC power supply was connected to the sample holder to increase the incoming ion energy and the positive electrode was grounded. The scheme of the two experimental configurations is shown in Fig 1. The deposition has been carried out with or without the DC power supply in order to study the effect of plasma assistance on the composition and properties of growing films especially in terms of nitrogen content and carbon hybridization. Before the deposition, the chamber was pumped until a base pressure of 10^{-4} Pa. The substrates were also carefully cleaned before introduction into the deposition chamber using successive ultrasonic baths of acetone and ethanol. A mass flow controller regulates the static pressure of N_2 flux at 10 Pa pressure for the films deposited by fs PLD and 5 Pa for fs-PLD films deposited with plasma using 250 V applied DC discharge voltage. For all the deposition conditions the laser fluence was kept constant to 5 J/cm^2. The experimental parameters are shown in Table 1. The thickness of the films, measured by a profilometer (Vecco Dektak), is controlled by the deposition time.

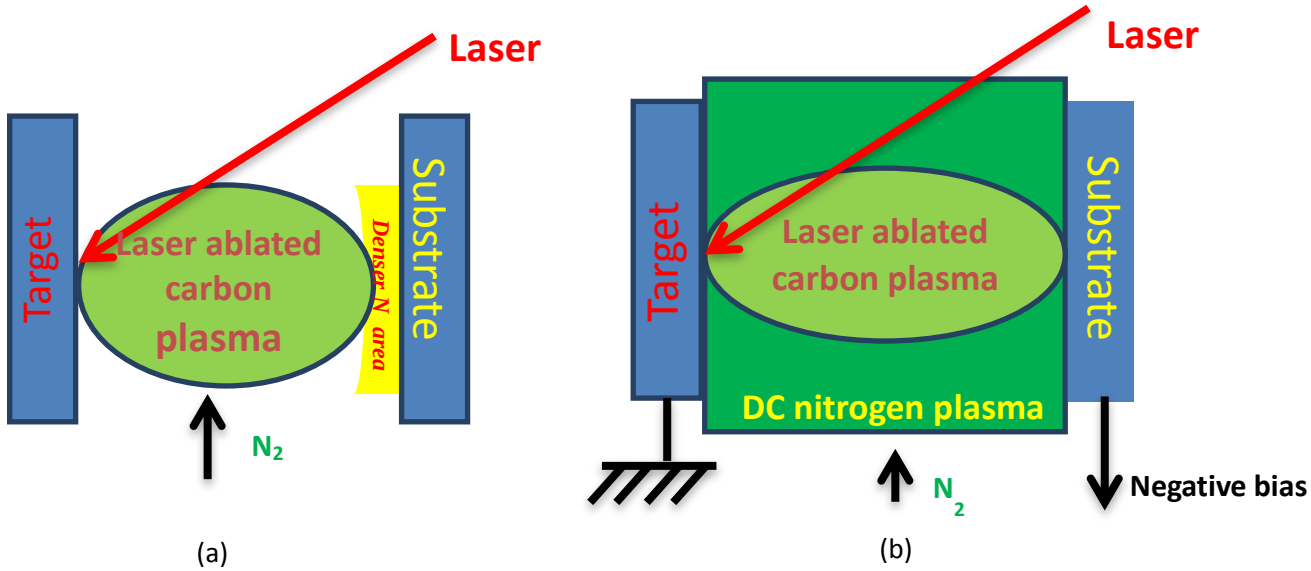

Fig.1. Schematic view of the deposition configuration a) without bias assistance, b) with bias assistance.

Table1. Experimental conditions for femtosecond PLD of films.

	a-C	a-C:N	biased a-C:N
Laser source	Ti: sapphire 800 nm		
Pulse width	60 fs		
Pulse energy	1 mJ		
Repetition rate	1 kHz		
Fluence	5 J/cm²		
Deposition rate	10 nm/min	2.5 nm/min	8 nm/min
N_2 pressure	-	10 Pa	5 Pa
DC biased voltage	-	-	250 V

Chemical surface analyses were carried out using X-Ray Photoelectron Spectroscopy. The analyses were performed with a Thermo VG Thetaprobe spectrometer instrument with a focused monochromatic AlKα source (hν = 1486.68 eV, 400 µm spot size). Photoelectrons were analyzed using a concentric hemispherical analyzer operating in the constant ΔE mode. The energy scale was calibrated with sputter-cleaned pure reference samples of Au, Ag and Cu in order that $Au4f_{7/2}$, $Ag3d_{5/2}$ and $Cu3p_{3/2}$ were positioned at binding energies of respectively 83.98, 386.26 and 932.67 eV. For all the samples analyzed, narrow scans were recorded for C1s, O1s and N1s with step size of 0.1 eV and pass energy of 50 eV. This pass energy gives a width of the $Ag3d_{5/2}$ peak measured on a sputter clean pure Ag sample of 0.55 eV. Components in C1s and N1s peaks were adjusted using lineshapes consisting of a convolution product of a Gaussian function (75%) and Lorentzian function (25%). Multi-Wavelength (MW) unpolarized Raman spectroscopy has been performed using an Aramis Jobin Yvon spectrometer at four different laser excitation wavelengths, namely, 325 nm, 442 nm, 488 nm and 633 nm. The spectral resolution was 2 cm^{-1}.

The laser beam has been focused on the sample with a confocal objective 40 X in UV and 100 X in visible. The power on the sample was kept below 10 mW for 633 nm radiation, 3.2 mW for 488 nm radiation, 2.8 mW for 442 nm radiation and 2.2 mW for 325 nm radiation, to avoid the laser induced degradation of films. The Raman signals have been acquired by a spectrometer equipped with a charge-coupled device (CCD) camera; all the spectra have been corrected by subtracting the normalized background spectrum with a similar silicon substrate. According to Ferrari, *et. al* [31], the Raman spectra were deconvoluted by a combination of an asymmetric Breit-Wigner-Fano (BWF) function for the G band, and a Lorentzian function for the D band and the C≡N stretch band observed at 2200 cm^{-1} for films deposited with plasma assistance. The TEM/EELS characterization was performed using a FEI FEG-TEM Tecnai G2 F30 S-Twin, equipped with a High Angle Annular Dark Field (HAADF) detector from Fischione Instruments, an SDD X-Max Energy-Dispersive X-ray spectrometer (EDX) detector from Oxford and a Imaging Filter EFTEM/EELS (GIF) model QUAMTUM SE.

3. Results and Discussion

The films surfaces were free of cracks and few particulates were observed, the particulates density increased very slightly with increasing of N content. The roughness (Ra) of films were obtained at scan area of 3 µm x 3 µm, the Ra of each film type was 2 nm (a-C), 6 nm (a-C:N) and 9 nm (biased a-C:N) respectively. The roughness values do not significantly increase with deposition conditions and remain in the same order of magnitude whatever the deposition conditions. XPS investigations allow the estimation of the chemical composition and carbon and nitrogen chemical environments at the topmost surface. The N content is found to be 14 and 28 at.% for the a-C:N and Biased a-C:N films, respectively. The N/C ratio of this deposited film is much higher than previously reported values obtained with nanosecond pulsed laser deposition with bias assistance [26]. Oxygen ranges between 8 and 12 at.% mainly due to adventitious surface contamination. The deconvoluted C1s and N1s spectra of pure a-C, a-C:N and biased a-C:N films are shown in Fig. 2. The binding energy values deduced from the C1s and N1s deconvolution spectra are summarized in Table 2. The pure a-C film shown in Fig. 2a exhibits two C1s components: C1 at 284.2 eV and C2 at 285.1 eV. A small shoulder at higher binding energy may be attributed to CO bonds due to adventitious surface contamination. Its low intensity does not allow to propose any significant fit to this contribution. The C1s and N1s spectra related to the a-C:N film (deposited at P_{N2} =10 Pa without any plasma assistance) are shown in Figs. 2b and 2d respectively. Two C1s components, at 284.3 and 285.3 eV, correlate well the C1 and C2 contributions found in pure a-C film. The intensity ratio of C1/C2 is significantly lower in the a-C:N compared to the pure a-C film. Additionally a C3 component centered at 287.3 eV may be attributed to CN bonds, due to the high electronegativity of nitrogen atoms. This

contribution may be also attributed to CO bonds, but its intensity is significantly higher when nitrogen is introduced into the film, compared to the pure a-C film. Even if the CO contribution exists, it remains weak and weakly overlaps the CC and CN contributions. Therefore it is ignored in the following discussion. The biased a-C:N film, deposited using DC plasma at P_{N2}= 5 Pa and a DC voltage of 250 V, exhibits C1s and N1s signal depicted in Figs. 2c and 2e respectively. The introduction of a bias, consistent with a nitrogen plasma assistance during the deposition, leads to subsequent decrease of the C1/C2 intensity ratio, along with a significant shift of 1 eV of the C1, C2 and C3 contributions. In addition, it is observed that the intensity of C3 strongly increases compared to the conventional a-C:N film. This is in favour to the attribution of the C3 component to CN bonds. The DC plasma assistance is clearly responsible for a multiplication by a factor two of the nitrogen content at a lower P_{N2} (5 Pa) compared to the film deposited in N_2 atmosphere with no DC assistance at higher P_{N2} (10 Pa).

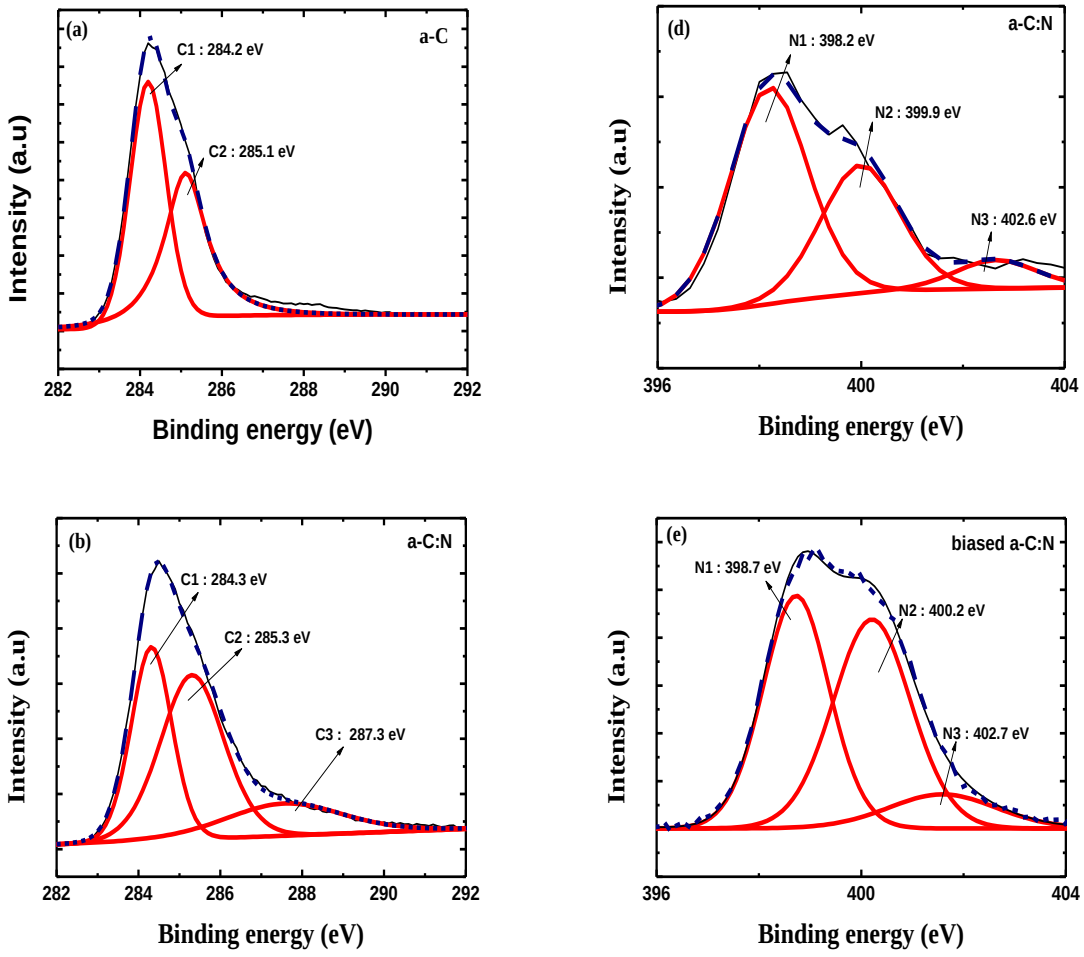

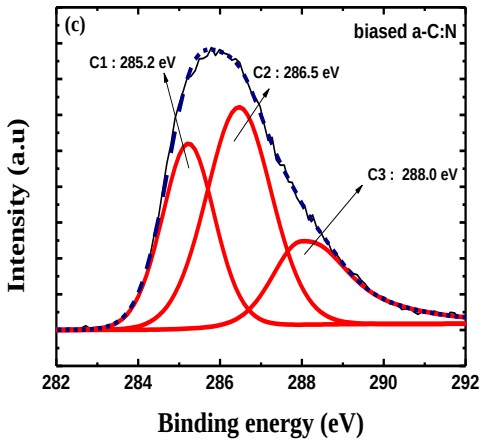

Fig.2. XPS deconvoluted C1s spectra of(a) a-C (b) a-C:N (c) biased a-C:N, and N1s spectra of (d) a-C:N, (e) biased a-C:N.

The nitrogen containing films exhibit three N1s contributions labeled N1, N2 and N3. The binding energy values for the different films are very similar, independently of the use or not of the plasma assistance, even if a small chemical shift of about 0.2-0.5 eV towards higher binding energies is observed with the DC plasma assistance. It is worth mentioning that the chemical shift related to different N-bonding environments is soundly lower than the chemical shift related to the C1s for the two nitrogenated films. N1 is centered at 398.2 – 398.7 eV, N2 is centered at 399.9 – 400.2 eV and N3 is centered at 402.6 – 402.7 eV. With plasma assistance, the N1/N2 ratio significantly decreases, whereas the N3 intensity slightly increases.

Table2. XPS C1s and N1s contributions in the a-C, a-C:N and biased a-C:N films and N/C ratio and N at.% deduced from XPS.

	$P(N_2)$ (Pa)	DC voltage (V)	C1 (eV)	C2 (eV)	C3 (eV)	N1 (eV)	N2 (eV)	N3 (eV)	N/C Ratio	N (at.%)
a-C	-	-	284.2	285.1	-	-	-	-	-	0
a-C:N	10	-	284.3	285.3	287.3	398.2	399.9	402.6	0.16	14
biased a-C:N	5	250	285.2	286.5	288.0	398.7	400.2	402.7	0.38	28

Since the sp^3, sp^2 and sp^1 hybridizations can exist for both C and N atoms, at least nine different bonding configurations can exist in carbon nitride films. Unambiguous interpretation of XPS is not possible by considering the literature data. Rodil *et al*. [29] have published a sound compilation of XPS data related to various CN films. Fig. 3 shows their conclusions on which our results have been superimposed.

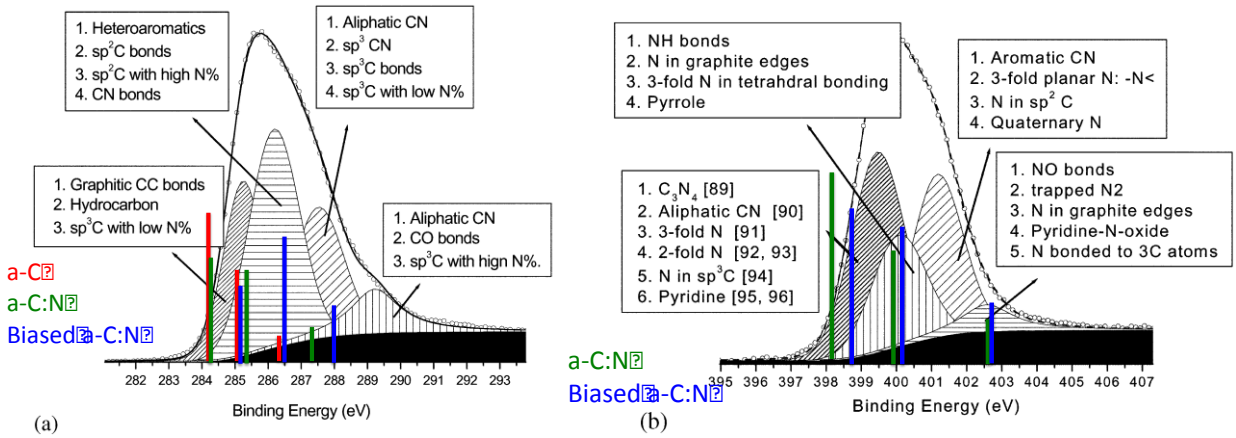

Fig.3. Chemical shifts of the C1s (a) and N1s (b) XPS spectra of a-C, a-C:N and biased a-C:N films superimposed on the compilation of Rodil *et al.* [29].

From Fig. 3, one can observe that the peaks of our XPS spectra are slightly but systematically shifted to lower binding energies, compared to the compilation of data from literature. This may be due to differences in energy calibration and charge shifts from one experimental configuration to another one. Such a shift does not prevent to go further in the discussion, since the acquisition has been performed in similar experimental conditions for all films. The a-C and a-C:N (14 at.%) have rather similar C1s contributions. According to the compilation published by Rodil *et al*. [29], the C1 peak may be affected mainly to carbon-carbon bonds (mainly Csp^2), but also to some Csp^3 bonds with low N concentration for the a-C:N film. Indeed it is known that our pure a-C films deposited by femtosecond PLD have Csp^2 content in the 60-70% range, compared to a-C films deposited by nanosecond PLD with a Csp^2 content in the 15-25% range [23]. The C2 contribution may be assigned to CN bonds in various possible configurations, including heteroaromatic rings containing N atoms for the a-C:N film. However, this C2 contribution is also observed in the pure a-C film, which is attributed by some authors to Csp^3 bonds. A chemical shift of less than 1 eV between two XPS peaks with a rather complex chemistry as for carbon is controversial. This indicates that a conventional attribution of the lowest energy contribution C1 only to CC bonds, and the higher energy contribution C2 only to CN bonds, in spite of a higher N

electronegativity compared to C, cannot fully explain the results. However the C1/C2 intensity ratio decreases when nitrogen is introduced, which is consistent with some possible assignations mentioned above: CN bonds can definitely explain part of the C2 contribution of the a-C:N film. The C3 peak may correspond to Csp^3 bonds in both films, including with low amounts of nitrogen, as well as aliphatic CN bonds. The three C 1s contributions of the biased a-C:N film (28 at.%) are significantly shifted towards higher binding energies. The C1 may correspond to carbon aromatic bonds, whereas the C2 should correspond to Csp^2 bonded to nitrogen. The increase of the C2 component is consistent with the increase of the nitrogen content up to 28 at.% due to plasma assistance. The C3 contribution can be related to Csp^3 bonds as well as aliphatic CN (including Csp^3-N bonds) or even CO bonds. Compared to the a-C film, the C2 and C3 contributions progressively increase from the a-C:N to the biased a-C:N films, consistent with their assignment to various types of CN bonds. The three nitrogen contributions N1, N2 and N3 are very similar for both nitrogenated films, with a decrease of N1 at the expense of N2 when DC plasma assistance is used. The interpretations compiled by Rodil *et al*. [29] indicate a sound difficulty to assess unambiguously the three nitrogen contributions. Schematically, the lowest N contribution may be attributed to Nsp^3-C bonds, whereas higher binding energies may be assigned rather to Nsp^2-C bonds. Such interpretations are consistent with a global increase of the aromatic character of our films when the nitrogen concentration is increased by bias assistance, with nitrogen predominantly incorporated inside aromatic carbon rings. Due to too much controversy related to the interpretations of XPS data of CN films in the literature, one concludes that XPS alone is not sufficient to elucidate the bonding states and their dependence versus the N content. EELS spectra allow to go further by probing the whole film thickness.

The EELS spectra of low and core-loss regions of pure a-C, a-C:N and biased a-C:N films are shown in Fig. 4. The low-loss part of the EELS spectra corresponds to collective excitations of valence electrons and may be correlated to the nature of the carbon bonds [32-34]. Fig. 4a shows the π-plasmon and the bulk plasmon peaks (Ep) located around 5.4 and 23 eV respectively. While the π-π* transition is almost invariable, the E_p value shifts about 1 eV when including N in the film composition. The E_p is known to vary from 33.3 eV for diamond, down to 25.5 eV for crystalline graphite and much lower for amorphous a-C with a predominance of sp^2 hybridization [23]. In the present study, the positions of the bulk plasmon peak shifts from 22.5 eV in pure a-C to 23.6 eV in both a-C:N or biased a-C:N samples, indicating an increased ordering of the amorphous Csp^2-bonded structures with the increment of the nitrogen content. These values are far from the characteristic value of diamond, confirming the non-predominance of sp^3 hybridized carbons [32, 34, 35]. We also observe that the values are lower than those published for crystalline graphite. This is consistent with a strong dependence of the plasmon energy values with the structural order in carbonaceous compounds. Also from the Fig. 4a, the increase in intensity of the π-

plasmon peak in the low-loss energy region with increasing the N content is consistent with more-ordered sp^2 graphitic domains.

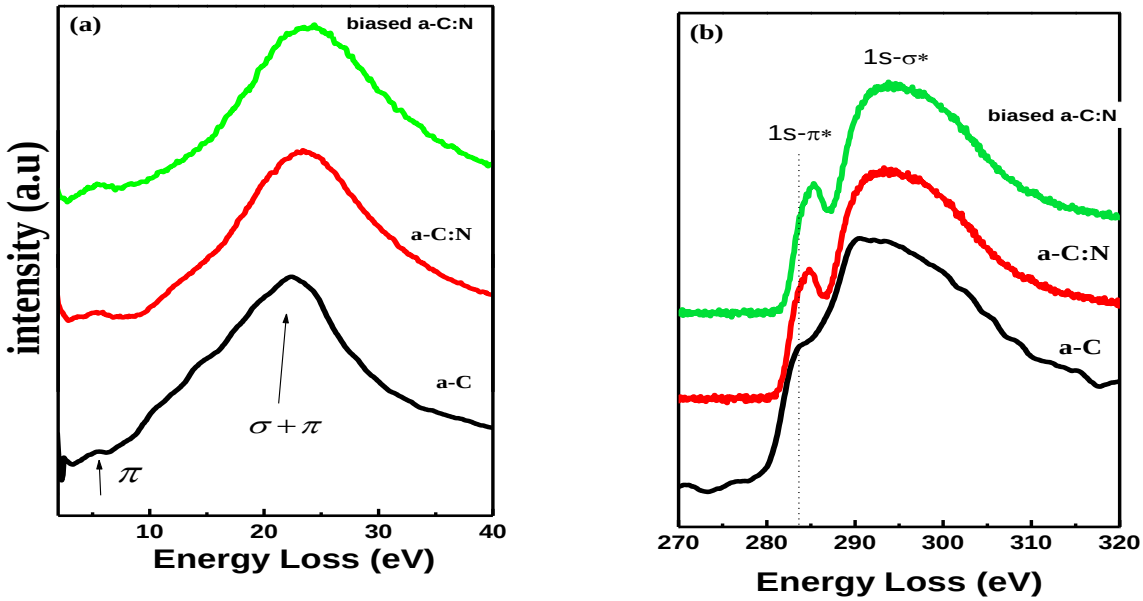

Fig.4. EELS spectra of the a-C, a-C:N and biased a-C:N films: (a) low loss spectra, (b) C-K edge spectra.

The C-K edge of the EELS spectra along with their π* and σ* regions of a-C, a-C:N and biased a-C:N films are shown in Fig. 4b. By increasing the N content, the peak due to C1s→π* transition is more defined and shifts from 283.6 eV in a-C to 284.7 eV in a-C:N, and 285.3 eV in biased a-C:N. The corresponding N contents deduced by EELS are 0, 17 and 24 at.%, respectively, in agreement with the XPS data reported in Table 2. This shift is attributed to a decrease of the electron density around carbon atoms originated by the higher electronegativity of nitrogen [36]. In general, π* peaks are not observed in tetrahedral bonded CN materials whose Csp^3-N bonds are denoted by the existence of small peaks at energy losses higher than 295 eV [36, 37]. The π* peak and the absence of peaks above 295 eV in the present CN films strongly suggest the predominance of sp^2 hybridized C bonded to N [30, 34-37], whereas no direct evidence of a Csp^2 increase due to the incorporation of nitrogen can be demonstrated by EELS investigations. The N-K edge spectra (not shown) are consistent with the 1s→π* and 1s→σ* transitions at 397.7 and 407.0 eV, respectively. According to the Rodil *et al*. [29], the interpretation of the N-K edge would be difficult due to the different configurations associated with N [29]. Fig. 5a, b and c show the MW-RAMAN analysis excited at four different wavelengths (325, 442, 488, 633 nm), for the a-C, a-C:N and biased a-C:N films respectively. Fig. 5d superimposes the spectra of the three films with an irradiation

at 325 nm. Table 3 summarizes the fitting parameters of all Raman spectra obtained at the four laser wavelengths for the three films. The D and G bands are characteristic of amorphous carbon based films and their positions are not clearly affected by the nitrogen content in the film, in agreement with [31]. Whatever the film, an increase of the G band position is observed with a decrease of the laser wavelength.

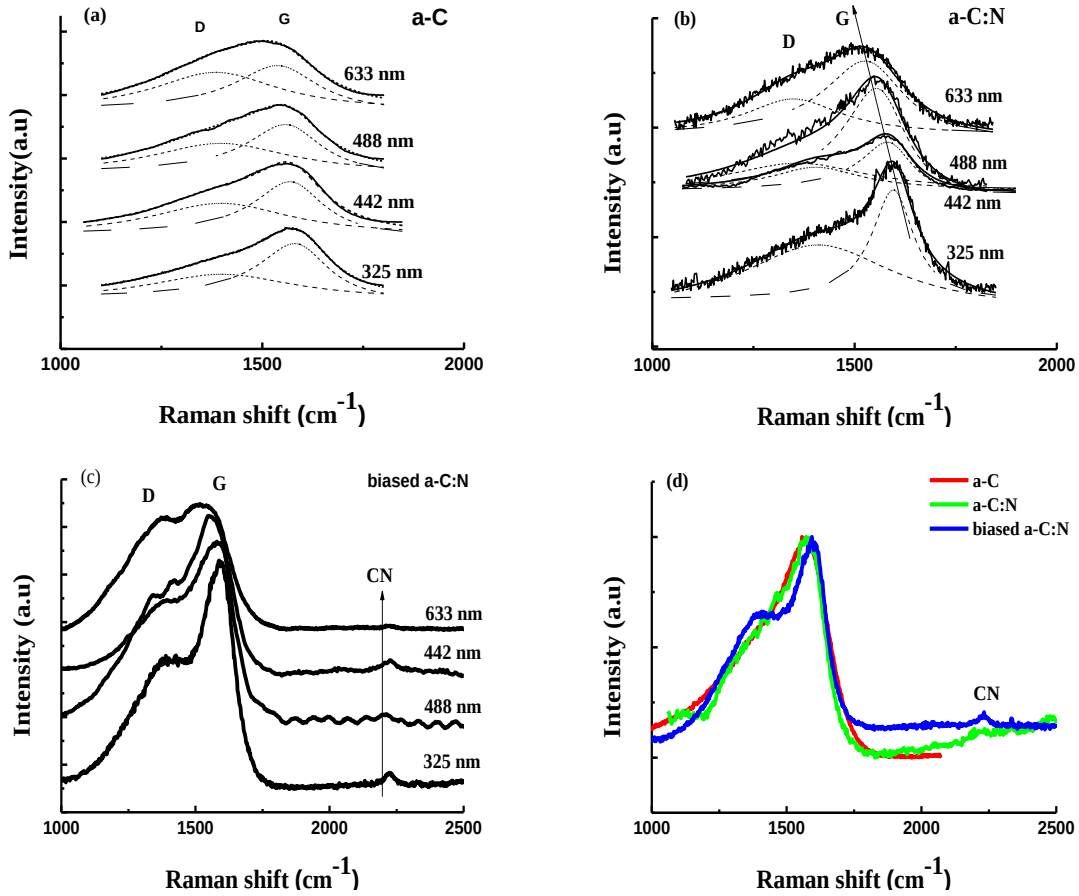

Fig.5. Raman spectra of (a) a-C, (b) a-C:N and (c) biased a-C:N obtained at four wavelength, (d) superimposed Raman spectra of the three films at 325 nm.

A band at 2225 cm^{-1} has been observed only with biased a-C:N film mainly for UV excitation, while it is barely detectable at higher wavelengths. This band corresponds to a terminal nitrogen triple bonded to carbon (C≡N), in agreement with the literature [31]. Even though it is not shown in Fig. 5b, the C≡N stretch band is not detected in a-C:N whatever the laser wavelength. The intensity ratio I(CN)/I(G) is only available for the biased a-C:N film, at 325 nm, 442 nm and 488 nm laser excitations. Indeed the 633 nm wavelength does not provide enough C≡N signal intensity to fit correctly the band. According to [31], a I(CN)/I(G) near 0.10 may correspond to nitrogen contents within 17-25 at% with some uncertainties. This order of magnitude is consistent with the composition of our biased a-C:N film. Indeed it is worth

mentioning that a minimum threshold of nitrogen is required to observe the C≡N band at 2225 cm^{-1}. This may indicate a kind of saturation in the incorporation ability of nitrogen in the carbonaceous network, leading to C≡N terminal groups at the highest nitrogen concentration. In the present study, this threshold is between 14 at.% and 28 at.%.

Table 3. Characteristics of MW Raman spectra related to the a-C, a-C:N and biased a-C:N films.

Sample	a-C				a-C:N				biased a-C:N			
Laser Wavelength(nm)	633	488	442	325	633	488	442	325	633	488	442	325
G position (cm^{-1})	1510	1556	1567	1573	1538	1565	1586	1595	1544	1563	1584	1597
G FWHM (cm^{-1})	300	227	206	208	197	159	146	139	190	154	140	136
D position (cm^{-1})	1362	1396	1397	1382	1386	1407	1441	1409	1361	1383	1403	1391
I(D)/I(G)	0.45	0.62	0.60	0.30	0.68	0.53	0.55	0.40	1.36	0.55	0.45	0.47
I(CN)/I(G)	-	-	-	-	-	-	-	-	-	0.08	0.12	0.06
Disp(G)(cm^{1}/nm)	0.21				0.19				0.17			

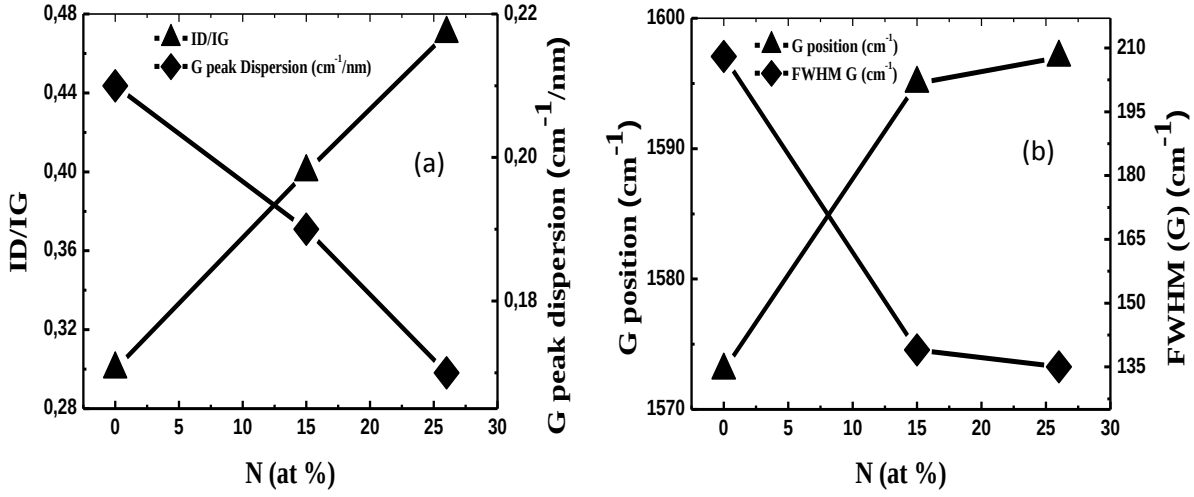

Fig.6. (a) Variation of I(D)/I(G) ratio and FWHM (G); (b) G peak position and G Peak dispersion versus N content deduced from RAMAN measurement at 325 nm.

The following discussion is mainly based on our results summarized in Fig. 6, considering the compilation of data interpretation proposed by Ferrari *et al.* [31]. The maximum values are recorded at 325 nm. No G band position exceeds 1600 cm^{-1}, which is consistent with a predominance of Csp^2 rings in all films. In

our previous study related to the pure a-C films, we observe a similar result with femtosecond PLD, whereas the films obtained by nanosecond PLD had a predominance of Csp^2 chains [23]. The G band shifts to higher values with increasing N content in agreement with previously reported data [18, 38]. This increment of G position together with an increase of D band intensity is attributed to an increase of Csp^2 clustering when the nitrogen content increases. The dispersion of the G band (Disp(G)) is related to the topological disorder, which corresponds to the size and shape distribution of rings. The dispersion of the G band is decreasing with increasing N content in films, from 0.21 to 0.17. These values are consistent with those obtained with other CN films, as reported on Fig. 7. A lower Disp(G) always means ordering of the film structure, which is consistent with the conclusion deduced from the increase of the G position with N content, as discussed above.

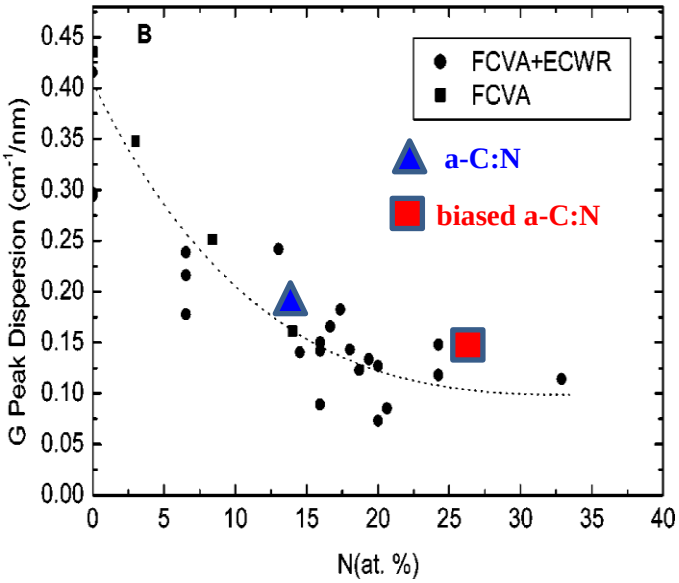

Fig.7. Dispersion of the G peak versus N content (already published data from [31]).

The FWHM of the G band is related to the structural disorder, which corresponds to the bond length and bond angle distortion of Csp^2 clusters. It is well known that FWHM(G) decreases when the excitation wavelength decreases. More interesting is to observe a decrease of FWHM(G) when the nitrogen content increases, which is consistent with a substantial loss of bond length and bond angle distortions of the clusters when the nitrogen content is high. The I(D)/I(G) ratio increases with increasing the N content for all excitation wavelengths. The increasing trend of I(D)/I(G) ratio is related to an increase in the

proportion of graphitic clusters [4, 29, 31]. Ferrari *et al*. [39] have proposed a relation between I(D)/I(G) ratio and the correlation length L_a, which is valid for crystallize size smaller than 2 nm.

$$I(D)/I(G) = C(\lambda) L_a^2 \quad (1)$$

C_2 (λ) is a constant which depends on the laser wavelength [40]. According to this reference, the value of C_2 (633 nm) is 8.2 nm. From the above relation, we estimated a correlation length L_a of 0.23 nm for a-C, 0.29 nm for a-C:N and 0.41 nm for biased a-C:N. The increase of aromatic cluster size with N content is consistent with reported data [15, 18, 31] as well as with other Raman parameters discussed above.

By crossing results from XPS, EELS and MW Raman, we can conclude an increase of the nitrogen content from 14 at.% (XPS) – 17 at.% (EELS), for the a-C:N film, to 28 at.% (XPS) – 24 at.% (EELS) for the biased a-C:N film. The increase of N content is associated to an increase of the clustering of the sp^2 phase in ordered rings of the CN films, developing more ordered graphitic clusters both in terms of structural and topological. The correlation length L_a of the clusters increases from 0.23 with no nitrogen incorporation, to 0.29 and 0.41 for the a-C:N and biased a-C:N films. On the basis of the extensive films characterization presented above, it is difficult to address without any doubt the growth mechanism of a-C:N films by PLD either under N_2 pressure or with the help of plasma assistance. The adhesion of thin films is always a critical parameter which has appeared to be degraded by the incorporation of nitrogen in amorphous carbon films [46]. Whatever the process used here, namely reactive fs-PLD or plasma assisted fs-PLD, the adhesion of a-C:N films is very good, in accordance with well-known results already observed in femtosecond-PLD [47]. Concerning the mechanism of nitrogen incorporation, one can obviously predict an increase in activation and reactivity of nitrogen with the help of the nitrogen plasma assistance resulting in CN formation in the carbon plasma induced by laser ablation. The additional energetic electrons generated in the plasma through the plasma assistance will increase the effective collisions probability and promote both the activation of N_2 molecules and radical formation. Even if the general features of films growth are driven differently for fs-PLD and ns-PLD [48], the use of fs-PLD under N_2 pressure and plasma assistance does not lead to significant different atomic bonding results compared to the use of nanosecond laser. In particular C≡N bonds are observed under plasma assistance in both conditions [12]. However we observe an increase of 19% of the N/C ratio by fs-PLD (0.38, see Table 1), compared by ns-PLD (0.32, see [12]). To go deeper in the analysis of growth mechanism a full characterization of the plasma induced under N_2 pressure and plasma assistance should be carried out. Moreover, the a-C:N materials with high nitrogen content and more graphite-like structure have to be characterized in order to address their electrochemical behavior. Such a-C:N with high nitrogen content and high structural and topological orders of the graphitic domains deposited by fs-PLD could be an

alternative to boron-doped diamond electrode in the near future. Particularly, its low temperature deposition allows the deposition onto polymer substrates towards environmental friendly applications.

4. Conclusions

Effects of DC polarized substrate during ablation of a graphite target by femtosecond pulsed laser ablation in an atmosphere of nitrogen on the structure and composition of the a-C:N film have been investigated in this study. The main conclusions are summarized as follows:

- Up to 28 at.% of nitrogen has been introduced in the a-C:N film by combining femtosecond laser ablation of graphite with a DC bias applied on the substrates. Such a high percentage has never been obtained by fs-PLD process.
- By comparing our XPS results with XPS data compilations, the exact interpretations of the C1s and N1s components are controversial due to rather complex chemistry of CN compounds with rather limited chemical shifts in the 1-2 eV range for both elements.
- By combining XPS, EELS and RAMAN results, the increase of nitrogen content can be associated to an increase of the aromatic character of the carbon network, by increasing the structural and topological orders of the graphitic clusters which certainly contain incorporated nitrogen.
- No clear and unambiguous evidence of Csp^2:Csp^3 dependence with the N content can be deduced.
- At the highest nitrogen concentration, terminal C≡N groups are incorporated in the film, which are observed only for plasma assisted-PLD, as already observed with longer laser pulse duration.

Acknowledgments

This work is produced with the financial support of the Future Programme Lyon Saint-Etienne (PALSE) from the University of Lyon (ANR-11-IDEX-0007), under the "Investments for the Future" program managed by the National Agency Research (ANR).

References

[1] A. Y. Liu, M.L. Cohen, Science, 245 (1989) 841-842.

[2] A. Y. Liu, R. M. Wentzcovitch, M.L. Cohen, Phys. Rev. B, 39 (1989) 1760-1765

[3] C. Donnet, A. Erdemir, Tribology of Diamond Like Carbon Films, Springer, New York, 2008.

[4] P. Wang, T. Takeno, J. Fontaine, M. Aono, K. Adachi, H. Miki, T. Takagi, Materials Chemistry and Physics, 145 (2014) 434-440.

[5] G. A. J. Amaratunga, S.R.P. Silva, Appl. Phys. Lett, 68 (1996) 2529-2531.

[6] B. S. Satyanarayana, A. Hart, W. I. Milne, J. Robertson, Appl. Phys. Lett, 71 (1997) 1430-1432.

[7] B. Khadro, A. Sikora, A.S. Loir, A. Errachid, F. Garrelie, C. Donnet, N. Jaffrezic-Renault, Sensors and Actuators B: Chemical, 155 (2011) 120-125.

[8] J. C. Byers, P. Tamiasso-Marthinhon, C. Deslouis, A. Pailleret, O.A. Semenikhin, J. Phys. Chem. C 114 (2010) 18474-18480.

[9] A. Zheng, V. F. Neto, J. J. Gracio, Q.H. Fan, Diamond Relat. Mater, 43 (2014) 12-22.

[10] Y. Miyajima, G. Adamopoulos, S. J. Henley, V. Stolojan, Y. Tison, E. Garcia-Caurel, B. Drevillon, J. M. Shannon, S.R.P. Silva, J. Appl. Phys, 104 (2008) 063701.

[11] G. Adamopoulos, C. Godet, C. Deslouis, H. Cachet, A. Lagrini, B. Saidani, Diamond Relat. Mater, 12 (2003) 613-617.

[12] E. Cappelli, S. Orlando, D. M. Trucchi, A. Bellucci, V. V, A. Mezzi, S. Kaciulis, Appl. Surf. Sci, 257 (2011) 5175-5180.

[13] P. Wang, T. Takeno, K. Adachi, H. Miki, T. Takagi, Appl. Surf. Sci, 258 (2012) 6576-6582.

[14] J.C. Sanchez-Lopez, M. Belin, C. Donnet, C. Quiros, E. Elizalde, Surf. Coat. Technol, 160 (2002) 138-144.

[15] B. Zhou, X. Jiang, A.V. Rogachev, R. Shen, D. Sun, D.G. Pilipstou, L. Lu, Appl. Surf. Sci, 287 (2013) 150-158.

[16] M.D. Tucker, Z. Czigany, E. Broitman, L.-A. Naslund, L. Hultman, J. Rosen, J. Appl. Phys, 115 (2014) 144312

[17] Ishpal, O.S. Panwar, M. Kumar, S. Kumar, Appl. Surf. Sci, 256 (2010) 7371-7376.

[18] R. McCann, S.S. Roy, P. Papakonstantinou, J.A. McLaughlin, J. Appl. Phys, 97 (2005) 073522.

[19] N. Benchikh, C. Debiemme-Chouvy, H. Cachet, A. Pailleret, B. Saidani, L. Beaunier, M.H. Berger, C. Deslouis, Electrochimica Acta, 75 (2012) 131-138.

[20] X. Yan, T. Xu, G. Chen, S. Yang, H. Liu, Q. Xue, J. Phys. D : Appl. Phys, 37 (2004) 907-913.

[21] C. Niu, Y.Z. Lu, M. Lieber, Science, 261 (1993) 334-337.

[22] Y. Aoi, K. Ono, E. Kamijo, J. Appl. Phys, 86 (1999) 2318-2322

[23] A. Sikora, F. Garrelie, C. Donnet, A.S. Loir, J. Fontaine, J.C. Sachez-Lopez, T.C. Rojas, J. Appl. Phys, 108 (2010) 113516.

[24] S. Muhl, J.M. Mendez, Daimond Relat. Mater, 8 (1999) 1809-1830

[25] Y.H. Cheng, X.L. Qiao, J.G. Chen, Y.P. Wu, C.S. Xie, S.B. Muo, Y.B. Sun, B.K. Tay, Appl. Phys. A, 74 (2002) 225-231.

[26] Y.H. Cheng, Z.H. Sun, B.K. Tay, S.P. Lau, X.L. Qiao, J.G. Chen, Y.P. Wu, C.S. Xie, Y.Q. Wang, D.S. Xu, S.B. Mo, Y.B. Sun, Appl. Surf. Sci, 182 (2001) 32-39.

[27] Y.H. Cheng, X.L. Qiao, J.G. Chen, Y.P. Wu, C.S. Xie, Y.Q. Wang, D.S. Xu, S.B. Mo, Y.B. Sun, Surf. Coat. Technol, 160 (2002) 269-276.

[28] Y.H. Cheng, X.L. Qiao, J.G. Chen, Y.P. Wu, C.S. Xie, Y.Q. Wang, D.S. Xu, S.B. Mo, Y.B. Sun, Diamond Relat. Mater, 11 (2002) 1511-1517.

[29] S.E. Rodil, S. Muhl, Diamond Relat. Mater, 13 (2004) 1521-1531

[30] J.C. Sanchez-Lopez, C. Donnet, F. Lefebvre, C. Fernandez-Ramos, A. Fernandez, J. Appl. Phys, 90 (2001) 675-681.

[31] A.C. Ferrari, S.E. Rodil, J. Robertson, Phys. Rev. B, 67 (2003) 155306

[32] E. Riedo, F. Comin, J. Chevrier, A.M. Bonnot, J. Appl. Phys, 88 (2000) 4365-4370.

[33] G. Soto, E.C. Samano, R. Machorro, M.H. Farias, L. Cota-Araiza, Appl. Surf. Sci, 183 (2001) 246-258.

[34] C. Spaeth, M. Kiihn, F. Richter, U. Falke, M. Hietschold, R. Kilper, U. Kreissing, Diamond Relat. Mater, 7 (1998) 1727-1733.

[35] C. Donnet, J.M. Martin, J. Fontaine, J.C. Sanchez-Lopez, C. Quiros, E. Elizalde, J.M. Sanz, T.C. Rojas, A. Fernandez, Surf. Coat. Technol, 120-121 (1999) 594

[36] J.C. Sanchez-Lopez, C. Donnet, M. Belin, T.L. Mogne, F.-R. C, M.J. Sayagues, A. Fernandez, Surf. Coat. Technol, 133-134 (2000) 430.

[37] A. Fernandez, P. Prieto, C. Quiros, J.M. Sanz, J.M. Martin, B. Vacher, J. Appl. Phys, 69 (1996) 764-766

[38] S. Prawer, K.W. Nugent, Y. Lifshitz, G.D. Lempert, E. Grossman, J. Kulik, I. Avigal, Diamond. Relat. Mater, 5 (1996) 433-438.

[39] A.C. Ferrari, J. Robertson, Phys. Rev. B, 61 (2000) 14095.

[40] M.J. Mathews, M.A. Pimenta, G. Dresselhaus, M.S. Dresselhaus, M. Endo, Phys. Rev. B, 59 (1999) 6585-6588.

[41] S. Bhattacharyya, C. Cardinaud, G. Turban, J. Appl. Phys

83 (1998) 4491.

[42] T.W. Scharf, R.D. Ott, D. Yang, J.A. Barnard, J. Appl. Phys, 85 (1999) 3142-3154.

[43] S.S. Roy, R. McCann, P. Papakonstantinou, P. Maguire, J.A. McLaughlin, Thin Solid Film, 482 (2005) 145-150.

[44] S.S. Roy, P. Papakonstantinous, R. McCann, J. McLaughlin, A. Klini, N. Papadogiannis, Appl. Phys. A, 79 (2004) 1009-1014.

[45] C. Ronning, H. Fledermann, R. Hofasaa, P. Reinke, J.U. Thile, Phys. Rev. B, 58 (1992) 2207-2215

[46] S. Peponas, M. Benlahsen, M. Guedda, J. Appl. Phys, 106 (2009) 013525

[47] A.-S. Loir, F. Garrelie, C. Donnet, J.L. Subtil, M. Belin, B. Forest, F. Rogemond, P. Laporte, Appl. Surf. Sci, 247 (2005) 225-231.

[48] Z. Zhang, P.A. VanRompay, J.A. Nees, R. Clarke, X. Pan, P.P. Pronko, Appl. Surf. Sci, 154-155 (2000) 165-171.